75th International Astronautical Congress (IAC) 2024 – Milan, Italy

IAC-24-A3,5,6,x84588

Modeling and Analysis of Tethered System Dynamics for Venus Aerobots and Towed Probes

Pierluigi Vergari[1*], Matteo De Matteis[1*], Marco B. Quadrelli[2], Richard Blomquist[2], Federico Rossi[2], Riccardo Apa[1], Stefano Aliberti[1], and Marcello Romano [1]

[1] *Astrodynamics & Advanced Orbital Systems Laboratory (ASTRADORS), Politecnico di Torino, Italy*

[2] *Jet Propulsion Laboratory, California Institute of Technology, Pasadena, CA, USA*

[*]Corresponding author
Email: pierluigi.vergari@polito.it, matteo.dematteis@polito.it

Abstract

Venus, the Earth's nearest planetary neighbor, provides a unique natural laboratory for studying planetary and climate processes. Because of its corrosive atmosphere, high temperatures, and pressures, Venus's atmosphere represents an extreme and challenging environment for scientific exploration. One of the most promising approaches to studying the Venusian atmosphere and its surface is to use an "aerobot" carrying scientific instruments. An aerobot is an autonomous buoyant balloon that could navigate Venus's atmosphere, staying at an altitude of around 52 km where temperatures and pressures are comparable to Earth's troposphere. This paper introduces mechanical models and flight simulators, developed to evaluate various system architectures to support the technological development of a possible Venus Aerobot mission. Two different modeling approaches of the tether dynamics are considered, specifically a Lumped-Mass approach and the Decoupled Natural Orthogonal Matrix (DeNOC) recursive approach. The models and simulators described in this paper enable preliminary system-level analysis of the flight-chain dynamics, encompassing inflated balloons, gondolas suspended by tethers, and bodies towed with tethers.

Keywords: Venus, Aerobot, Tethered Systems, Multi-body Dynamics, Flight Mechanics, Simulation, Space Robotics, Planetary exploration, Towed Body Dynamics.

1. Introduction

Venus, often described as Earth's twin due to its similar size and composition, presents a fascinating yet extreme environment for scientific studies. Unlike Earth, Venus has experienced a runaway greenhouse effect, resulting in surface temperatures exceeding 450 degrees Celsius and atmospheric pressures 91 times higher than Earth's and making Venus the hottest planet in the solar system. These characteristics offer a unique example to understand the dynamics of planetary atmospheres and the mechanisms driving climate change [1]. Despite its inhospitable conditions, Venus is a prime candidate for exploration due to its potential to reveal insights into planetary evolution, atmospheric science, and conditions that might support life. One of the most promising methods for exploring Venus involves using autonomous aerostatic balloons, known as aerobots [2]. These vehicles can float in the relatively mid-upper atmosphere, around 52 km altitude, where atmospheric conditions resemble those found on Earth.

The Venus Aerobot project, lead by NASA's Jet Propulsion Laboratory, aims to develop a mission that can withstand and operate in the extreme conditions of Venus. This paper introduces mechanical models and a flight simulator which were designed to support the development and testing of the Venus Aerobot mission. The simulator is a critical tool for evaluating various system architectures and mission scenarios, ensuring that the aerobot can navigate in Venus's atmosphere.

Two dynamic modeling approaches are considered:

the Lumped-Mass method [3] and the Decoupled Natural Orthogonal Complement (DeNOC) technique [4]. These models enable simulating the aerobot's dynamics with high accuracy, taking into account the complex interactions between the balloon, tether, and towed bodies. Additionally, the simulator incorporates a stochastic wind model to replicate the unpredictable atmospheric conditions on Venus, providing a robust framework for mission planning.
The flight simulator serves multiple purposes, including design parameter optimization, system performance prediction, and mission concept testing. One such concept includes the use of towed atmospheric probes, which can extend the scientific reach of the mission by sampling lower atmospheric layers and surface materials. The simulator's ability to model these scenarios and the integration of autonomous Micro Aerial Vehicle (MAV) for tracking towed bodies further enhance its utility.
In summary, the Venus Aerobot flight simulator is a vital tool for the successful planning and execution of Venus exploration missions. It offers a comprehensive platform for understanding the dynamics of aerobot systems and supports the development of innovative mission strategies.

The main contributions of the paper are:

1. Performance comparison of two dynamic modeling approaches, Lumped-Mass and DeNOC, for dynamical analyses of tethered systems.
2. Dynamics and performance analyses of aerobot architectures for planetary scientific exploration, emphasizing towed body configurations.
3. Demonstration of trajectory change feasibility for a towed body system by differential aerodynamic forces between the balloon and the gondola in a Venusian operational environment.
4. Demonstration of rendezvous and docking a small drone (MAV) with the gondola.

The paper is organized as follows. Sec. 2 gives an overview of aerobot systems, dealing with their architecture and materials. Sec. 3 addresses aerobot and operational environment modeling, introducing the two dynamic modeling approaches, the external forces acting on the system, and the stochastic wind model employed. Sec. 4 gives insights into flight simulator architecture, presenting significant case studies. Sec. 5 refers to the towing problem, a system architecture of high scientific importance that has been employed in studies of system trajectory variation and gondola tracking. Finally, Sec. 6 presents the conclusions and future studies.

2. Overview on Aerial Robots

Aerobots, or aerial robots, offer a promising solution for exploring Venus's dense and hostile atmosphere. These vehicles utilize buoyancy to maintain stable altitudes, making them ideal for scientific missions in extreme environments. This section provides an overview of the aerobot system, including its architecture, materials, and a reference prototype, while highlighting its suitability for Venus exploration.
The aerobot system is the combination of three main components: a balloon, tethers and payloads. The balloon is filled with a lower density gas such as helium to provide lift and maintain a stable altitude between 52 and 60 km where temperatures and pressures are more manageable. The tether connects the balloon to the payload, which houses scientific instruments and control systems, enabling the aerobot to collect valuable atmospheric and surface data.
Several aerobot architectures have been proposed to optimize performance and survivability in Venus's extreme conditions [5, 6]. The Pumped Helium configuration is preferred for Venus missions due to its simplicity and efficient altitude control capabilities. This architecture allows the aerobot to navigate a wide range of altitudes without significant helium loss or ballast release.
Material selection is crucial for the aerobot's durability and performance. Helium is used for its low density, high lifting capacity, chemical inertness, and thermal stability, essential for withstanding Venus's corrosive and high-temperature atmosphere. The balloon is typically constructed with a metalized, vapor-deposited, Fluorinated Ethylene Propylene (FEP) layer bonded to a structural plastic material like Kapton or Mylar. The FEP layer offers resistance to sulfuric acid and reflects solar radiation, while the structural plastic provides strength and flexibility, reducing the risk of gas leakage and enhancing durability [7].

A notable reference prototype for the Venus Aerobot is the variable altitude aerobot developed by NASA's Jet Propulsion Laboratory and Near Space Corpora-

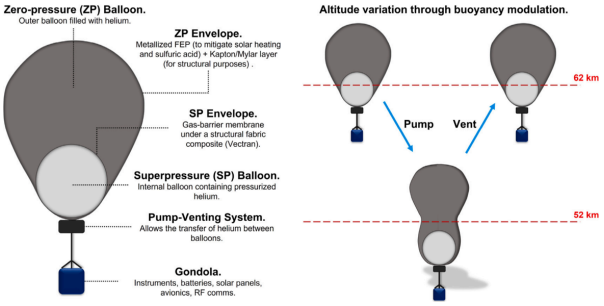

Figure 1: *Pumped Helium reference architecture and operation [8]*

tion [8, 5]. This prototype employs a two-part balloon system with an inner Superpressure balloon and an outer Zero-pressure balloon, facilitating efficient buoyancy modulation. The prototype, approximately one-third the scale of the intended mission balloon, measures about 4 meters in diameter and is designed to operate at altitudes between 52 and 62 kilometers. It incorporates advanced materials and manufacturing techniques to ensure resilience against Venus's harsh conditions, with the metallized FEP and structural plastic layers providing a robust envelope capable of withstanding solar heating and sulfuric acid exposure.

3. Aerobot dynamic modeling

Herein, the balloon and gondola are modeled as rigid bodies. Two different modeling approaches are employed for the tether elements, Lumped-Mass and DeNOC, which are detailed in the following sections. In this paper, the influence of temperature on the dynamics is not taken into account, and the balloon is assumed to be completely inflated and spherical (no transient inflation considered), hence also modeled as a rigid body.

3.1 Lumped-mass

The Lumped-Mass modeling is a state-of-the-art dynamical modeling approach for tethered systems. The method [9, 3] uses a Kelvin-Voigt representation that simplifies the continuous tether as a series of discrete point masses connected by massless springs and dampers, providing a manageable yet accurate representation of the system's dynamics as the number of masses increases and the distance between masses decreases, as shown in Fig.2. This section focuses on the Lumped-Mass modeling of the aerobot system, outlining the convention used for the flight simulator and the set of forces acting on the elements that constitute the system.

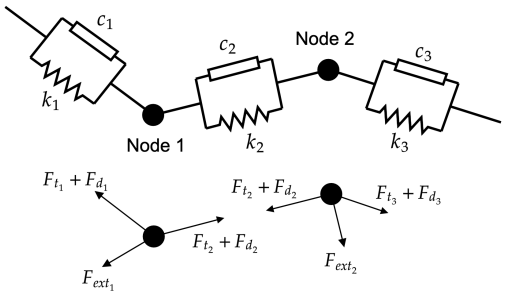

Figure 2: *Kelvin-Voigt tether scheme [3]*

3.1.1 Tether model

Using the Lumped-Mass approach, the tether is divided into N point masses interconnected by $N-1$ linear tether elements. Each tether segment is modeled as a Kelvin-Voigt element, thus acting as a spring-damper system, and the mathematical model is detailed in [3]. The tension ($\mathbf{F}_t$) and damping ($\mathbf{F}_d$) forces operate exclusively along the axis of each tether element defined in a three-dimensional space. The external forces ($\mathbf{F}_{ext}$), i.e. aerodynamics, act on the point mass. These forces are defined using the parameters stiffness ($k\left[\frac{N}{m}\right]$) and damping coefficient ($c\left[\frac{Ns}{m}\right]$). The former is a function of the Young's Modulus ($E[Pa]$), the tether area ($A_t[m^2]$) and the tether length ($l_t[m]$) through the equation $k = \frac{EA_t}{l_t}$, while the latter is more challenging to determine from the tether's primary material and structural properties. For this reason, an assumption of its value has been made. Since the two parameters depend on the tether element length, they are then computed as functions of the number of tether segments considered: $k_N = k(N+1)$ and $c_N = c(N+1)$.
Overall, each node in the Lumped-Mass model is composed of 6 states: the position and velocity of the node in the three-dimensional space. The tension force depends on the norm of the relative distance, and the damping force depends on the scalar product of the relative velocity with the relative position. Thus, the resulting system of equations will be highly non-linear in the system kinematic states.

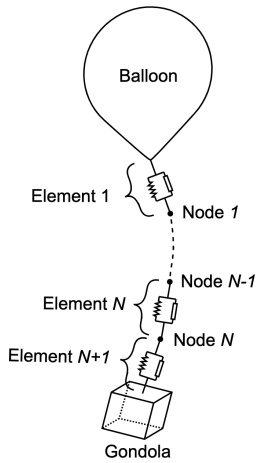

Figure 3: *Aerobot Lumped-Mass modeling [3]*

3.1.2 Rigid Bodies

As mentioned earlier, the balloon, gondola, and all other bodies connected to the flight chain are modeled using rigid body dynamics. Newton's second law is applied to the translational dynamics, resulting in a set of three equations of motion for each rigid body. The rotational motion of each rigid body is described by Euler's equations which generate a set of three equations written in the body reference frame. Although the problem is considered in 3-D, the tether masses do not exhibit attitude changes, so only Newton's second law is applied to them. Euler's equations, on the other hand, must be applied to any rigid body that exhibits attitude changes.

The differential kinematic equations required to determine the rigid body's attitude are derived through quaternion kinematics using a transformation [10]. The concept of product of quaternions is then applied by extending the angular velocity vector written in the body reference frame with a fourth null component $\hat{\boldsymbol{\omega}} = [p, q, r, 0]$, so that the kinematic differential equation for the quaternion is given by $\dot{\mathbf{q}} = \frac{1}{2}\mathbf{q} \otimes \hat{\boldsymbol{\omega}}$, where $\otimes$ represents the quaternion multiplication, $\dot{\mathbf{q}}$ the quaternion derivative, and $\mathbf{q}$ the quaternion.

Knowing the angular velocities from the sensors makes it possible to compute the quaternion and get the current attitude.

3.2 DeNOC

The Decoupled Natural Orthogonal Complement (DeNOC) modeling approach is a robotic-based recursive method used for the dynamic modeling of multi-body systems. It is particularly effective in reducing the computational complexity of such systems by decoupling the kinematic and dynamic equations, allowing for a more efficient calculation of the system's dynamics. DeNOC was implemented by exploiting the Space Robotics Tool (SpaRT) [11], a MATLAB open-source modeling and control toolkit for mobile-based robotic multibody systems with kinematic tree topologies. Starting from the system Denavit-Hartemberg parameters, the software solves the kinematics, dynamics, differential kinematics, and differential dynamics problems, characterizing the aerobot dynamics in the Venusian environment. The capability of the SpaRT software to dynamically model only systems having a kinematic tree architecture is a strong limitation for the DeNOC approach, which will be used only for modeling simple single-cable architectures.

3.2.1 Aerobot DeNOC modeling

Representing the aerobot as a robotic manipulator, the gondola is considered the base block of the architecture; from it, the dynamics of the whole system is recursively solved. The payload housing will then coincide with the base link $\mathcal{L}_0$ and, following that, the series of n links $\mathcal{L}_n$ connected by spherical joints will constitute the tether. The balloon, being the last element $\mathcal{L}_{n+1}$ in the kinematic chain, will constitute the end-effector of the manipulator.

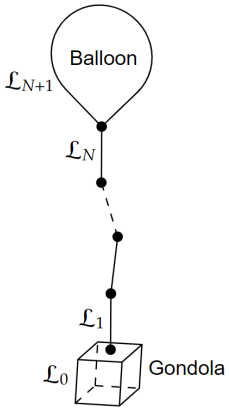

Figure 4: *Aerobot DeNOC modeling*

Each tether link is assigned geometric and inertia characteristics representative of the actual tether. The balloon, a rigid sphere whose diameter descends

from an equilibrium point design process in the Venusian atmosphere, supports the variable shape gondola via buoyancy force. For this study, the tether model using the DeNOC approach does not implement elasticity.

Given a Multi-body system (MBS) consisting of n joints and $n+1$ links, the system Newton-Euler equations can be written as:

$$\mathbf{M}\dot{\mathbf{t}} + \dot{\mathbf{M}}\mathbf{t} = \mathbf{w} \ , \tag{1}$$

where $\mathbf{M} \in \mathbb{R}^{6(n+1)\times 6(n+1)}$ is the MBS mass matrix, containing information about the inertial properties of the links; $\mathbf{t}, \dot{\mathbf{t}} \in \mathbb{R}^{6(n+1)\times 1}$ are, respectively, the system twist matrix and twist rate, containing the MBS links velocities and accelerations; $\mathbf{w} \in \mathbb{R}^{6(n+1)\times 1}$ is the system wrench column matrix, a set of wrenches acting on the system that can be decomposed into a work-contributing $\mathbf{w}^c$ and a non-work-contributing $\mathbf{w}^n$ part.

The Saha method within the DeNOC framework significantly reduces computational effort by enabling the construction of the Natural Orthogonal Complement (NOC), i.e. the system Jacobian Matrix $\mathbf{N} \in \mathbb{R}^{6(n+1)\times(6+n)}$. The part of the wrenches that do not contribute to the total work of the system can be eliminated by pre-multiplying the transpose of the above matrix $\mathbf{N}^T$ to the equations of motion

$$\mathbf{N}^T(\mathbf{M}\dot{\mathbf{t}} + \dot{\mathbf{M}}\mathbf{t}) = \mathbf{N}^T\mathbf{w}^c \ . \tag{2}$$

Then, by exploiting kineto-static duality, it is possible to obtain the system equations of motion in the joint space, a mathematical representation of all possible configurations of a MBS in terms of its n joint variables:

$$\mathbf{H}\dot{\mathbf{u}} + \mathbf{C}\mathbf{u} = \boldsymbol{\tau} \ , \tag{3}$$

where $\mathbf{H} \in \mathbb{R}^{(n+6)\times(n+6)}$ is the system inertia matrix; $\mathbf{C} \in \mathbb{R}^{(n+6)\times(n+6)}$ is the convective inertia matrix; $\mathbf{u}, \dot{\mathbf{u}} \in \mathbb{R}^{(n+6)\times 1}$ are, respectively, the system joint-space velocities and accelerations; and $\boldsymbol{\tau} \in \mathbb{R}^{(n+6)\times 1}$ is the generalized force matrix.

The NOC matrix avoids the inertia matrix inversion when solving the system equations of motion and recursively solving the system dynamics. Please refer to [4] and [12] for a complete and detailed discussion of the Saha method.

3.3 External forces

This section introduces the external forces acting on the tether and the rigid bodies. The primary forces involved are aerodynamic and gravity ($g = 8.87m/s^2$) forces, which affect both the tether and the rigid bodies. In addition to these forces, the balloon is subject to buoyancy and the added mass effect caused by unsteady aerodynamic forces, which occurs when a large object moves through a fluid [13]. The added mass value is $m_{added} = \frac{2}{3}\rho\pi R^3$, where R is the sphere radius and ρ is the air density, which is added only to the body's inertia and not its weight, so that $\sum \mathbf{F}_i = (m_{balloon} + m_{added}) \cdot \mathbf{a}$.

The buoyant force, described by Archimedes' principle, further influences the balloon. This force is given by $\mathbf{F}_\text{b} = \rho_\text{air}(z) \cdot V_\text{balloon} \cdot \mathbf{g}$, where $\rho_\text{air}(z)$ is the air density at altitude z, V_balloon is the displaced volume, and $\mathbf{g}$ is gravity. The lower density of helium compared to air allows the balloon to rise and keep a desired altitude.

3.3.1 Aerodynamics effects

For the tether aerodynamics, the model used is explained in [14]. Typically, for discretized cables, aerodynamic forces are determined by calculating the drag generated on adjacent segments of the cable and then averaging the resulting force on the jth mass. Specifically, the drag force acting on the jth mass is calculated based on its velocity and the orientation of the $(j-1)$th cable segment. The accuracy of this approximation improves as the number of segments increases, particularly when the cable exhibits significant curvature.

For the balloon and all other rigid bodies, except the sail introduced in Sec. 5.2, only drag is considered; thus, lift is neglected and no aerodynamic moment is taken into account. The aerodynamic forces are applied at the body's center of mass, where the center of pressure coincides with the center of mass. Each body may have a different drag coefficient; for the balloon, the drag coefficient is considered Reynolds number-dependent [15]. The drag is modeled using the equation $\mathbf{D} = -\frac{1}{2} \cdot \rho_{air}(z) \cdot ||\mathbf{V}_{rel}|| \cdot C_d \cdot S_{ref} \cdot \mathbf{V}_{rel}$, where $\rho_{air}(z)$ is the air density at altitude z, $\mathbf{V}_{rel}$ is the relative velocity of the body with respect to the flow, C_d is the drag coefficient, and S_{ref} is the reference area.

3.4 Atmospheric Model

Understanding the thermodynamic properties of Venus's atmosphere is crucial for accurately modeling the aerobot's dynamics. The Venusian atmosphere is predominantly composed of carbon dioxide (96.5%), with traces of nitrogen (3.5%) and other gases including sulfur dioxide. For the purposes of this study, the atmosphere is simplified to consist solely of carbon dioxide to allow the use of the Sutherland formula for calculating atmospheric dynamic viscosity, which is a critical parameter in determining the Reynolds number. The Reynolds number, in turn, affects the aerodynamic behavior of the aerobot.
The model for atmospheric density, pressure, and temperature used in the simulations is derived from the Venus Climate Database [16, 17, 18], also employed by NASA's Jet Propulsion Laboratory. This database provides discrete values of these parameters across different altitudes, which are then interpolated to obtain continuous profiles.

3.5 Stochastic Wind Model

The stochastic wind model implemented in the simulation is intended to capture the probabilistic characteristics of Venusian winds [19], crucial for predicting the aerobot's response to atmospheric disturbances. This model is based on a set of Stochastic Differential Equations (SDEs), specifically using a two-dimensional Ornstein-Uhlenbeck (OU) process. The autocorrelation function (ACF) and the probability density function (PDF) are employed to replicate the memory effects and probabilistic nature of wind data. The ACF is expressed as:

$$R_X(\tau) = e^{-\alpha\tau}\cos(\omega\tau)\ , \tag{4}$$

where α and ω are model coefficients. The stochastic process incorporates Gaussian distributions for wind speed, modified through memoryless transformations to match observed wind distributions on Venus. The model allows for the realistic simulation of wind gusts and their impact on the aerobot, providing critical insights into its operational stability.

4. Venus Aerobot Simulator Design and Analysis

4.1 Simulator architecture

The simulator adopts a modular and user-friendly structure that allows the user to build complex system architectures in a few simple steps. The simulation process for both modeling approaches can be divided into three phases:

1. Pre-processing: definition of system characteristics and operating conditions on Venus.
2. Processing: system dynamic resolution.
3. Post-processing: Representation of results by plots and animations.

During the first phase, the user is asked to provide the geometric and inertial characteristics of the system, as well as the initial conditions in terms of altitude, route latitude and wind model to be used in the simulation. This will create the *aerobot* structure, the foundation of the simulation process. Starting from such a structure, the system's dynamics is simulated through an integration of the equations of motion forward in time. This will lead to the visualization of plots and animations of the motion in the post-processing stage.

4.2 Modeling approaches comparison

One of the primary objectives of this study was to compare the performance of two different modeling approaches: Lumped-Mass model and DeNOC. The comparison was executed using a test case involving a $900m$ tether discretized with 10 masses and a starting altitude of $56000m$, equal to the system's equilibrium altitude. The system was subjected to step gusts in different directions to assess the dynamic response. These wind gusts consist of a step gust in x direction $w_x = 5\ \frac{m}{s}$ from 10 to 20 s; a step gust in y direction $w_y = 3\ \frac{m}{s}$ applied between 18 and 35 s; and a step gust in z direction of $w_z = 5\ \frac{m}{s}$ from 50 to 60 s. Neither added mass for the balloon nor torsional response for the cable have been considered in this test case.
The results of the cross-validation showed that the trajectories of the system elements coincided in both modeling approaches. The displacements of the balloon and gondola in the x, y, and z directions were analyzed.

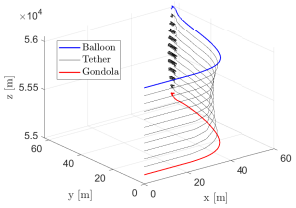

Figure 5: *Lumped-Mass system trajectory*

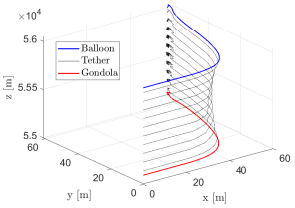

Figure 6: *DeNOC system trajectory*

4.3 Performance Study

A performance study was conducted to analyze the variation in the system's dynamic response as specific parameters were altered. Two test cases were considered:

1. Varying the number of elements constituting the tether from 1 to 20, while keeping the tether length constant at 1000 m, as shown in Fig. 7.
2. Varying the length of the tether from 50 m to 1550 m, while keeping the number of masses constituting the tether constant at 5 elements, as shown in Fig. 8.

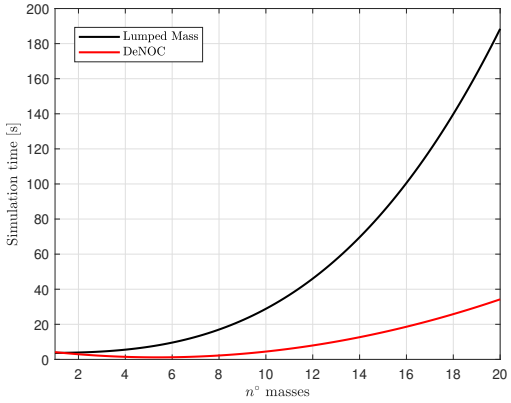

Figure 7: *n masses performance study*

The Lumped-Mass method was found to be of computational complexity $O(n^3)$, where n is the number of elements constituting the system. In contrast, the DeNOC method demonstrated a computational complexity of $O(n)$, making it more efficient for larger systems. Furthermore, the DeNOC approach was shown to be independent of the cable length parameter, unlike the Lumped-Mass model, which was strongly dependent on it due to the elasticity of the tether.

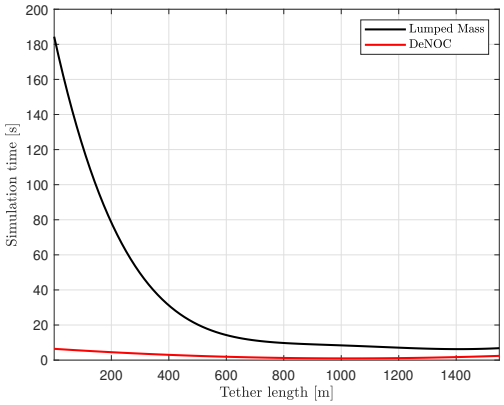

Figure 8: *Tether length performance study*

The comparison and performance study highlighted the potential of DeNOC for modeling the aerobot and tethered systems in general. Although the DeNOC model does not account for the elasticity of the tether, it successfully captures the macroscopic dynamic behavior of the system, making it a rapid and effective tool for preliminary mission studies.

4.3.1 Multi-tether and flight chain simulation capability

As previously mentioned, SpART does not allow the simulation of closed-loop chains, i.e., the case of more than one tether connected to the balloon and rigid bodies. Instead, closed-loop chains are simulated using the Lumped-Mass approach due to its versatility and modularity; some examples of simulated architectures are shown in Fig. 9 and Fig. 10. The multi-tether capability was needed to carry out analytical studies of the test conducted in the Mojave Desert by NASA's Jet Propulsion Laboratory team and to prove the origin of some phenomena, such as the pendulum-torsion coupling motion of the gondola experienced in the real-case, which will not be explained in this article. The tested tethered structure is shown in Fig. 11. The developed simulator is also capable of simulating more complex architectures involving mission-like instrumentation, such as magnetometers, microphones, or cameras that operate at a lower altitude and are connected to the gondola (or to each other) through a single- or multi-tether architecture. An example is shown in Fig. 10.

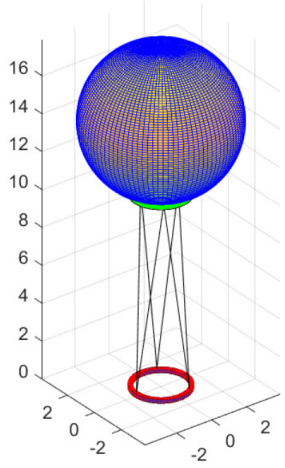

Figure 9: *Multi-tether architecture*

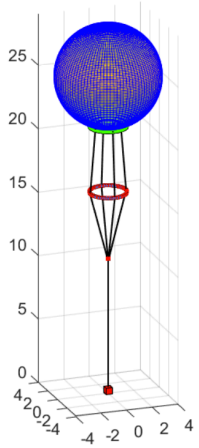

Figure 10: *Flight chain architecture*

Figure 11: *Mojave desert test - View from the Balloon to the Gondola [20]*

4.4 Validation for multi-tether architectures and sensitivity analysis

In this section, we describe a sensitivity study conducted with the developed simulator and compare the results with those obtained with a validated and open-source Multi-physics Dynamics Simulation Engine called *Project Chrono* [21]. In this study, the tether length is varied to understand if the response has a physical sense. The architecture considered is depicted in Fig. 12.

4.4.1 Tether length study

As anticipated before, in this section, a sensitivity study that involves changes in the tether length is described. For this study, the balloon is considered fixed, and the main parameters are $m_{body} = 20$ kg, which is the mass of the hanging body; Upper tether radius = 1 m, which is the radius of the circle that connects all the tether attachment points on the fixed balloon; Lower tether radius = 1 m, which is the radius of the circle that connects all the tether attachment points on the hanging body; $r_{ext} = 2.1$ m, $r_{int} = 1.3$ m and $h = 0.2$ m, which are the external radius, internal radius and thickness of the hollow cylinder.

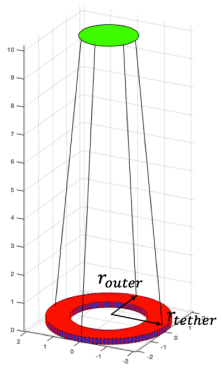

Figure 12: *System considered for the sensitivity analyses*

No wind is considered for this simulation, and an initial angular velocity $\omega_0 = 0.1$ rad/s along the z-axis is applied on the hanging body in order to study the response. The yaw angle is considered to analyze the system's torsional response. In Fig. 13, the yaw angle is reported as the tether length varies. As the tether length increases, the time to transmit the rotation from the bottom to the top of the tether and vice versa increases, indicating a physical result. Consequently, the oscillation period increases. An increase in amplitude is also detected as the tether length becomes longer.

To validate the results of the developed simulator in this analysis, the same analysis is conducted in Project Chrono. The patterns in Fig. 14 (Project Chrono) and the patterns in Fig. 13 (Simulator) are similar, with the small differences attributed to the numerical integrator used. In the Project Chrono results, numerical damping is evident after a certain amount of time. Additionally, a comparison in the frequency domain is presented in Tab. 1, from which it can be seen that the main frequencies are the same in both the conducted analyses.

5. Towing problem

The towing analysis is an important study done thanks to the versatility of the developed simulator.

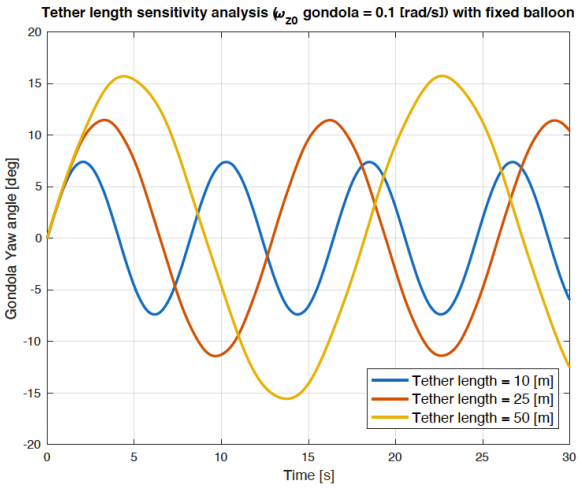

Figure 13: *Sensitivity analysis with the developed simulator involving changes in tether length – Time response*

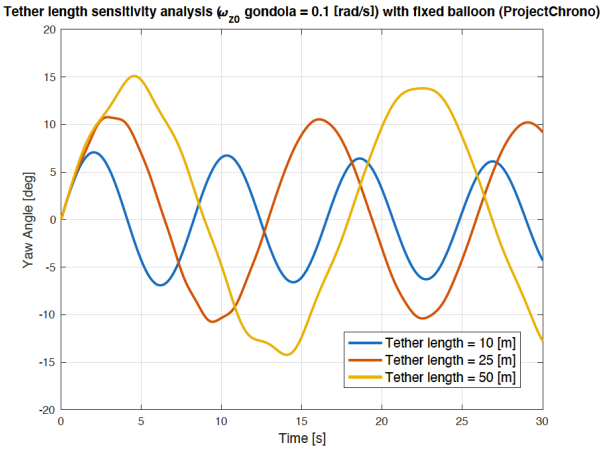

Figure 14: *Sensitivity analysis with Project Chrono involving changes in tether length – Time response*

In this particular system, long tether lengths from 900 m to 10000 m are considered, and a probe is attached at the bottom. In this way, the balloon will float at a high altitude, where the conditions are similar to the Earth, and the requirements for the material would be less strict. Instead, the probe will operate at a lower altitude with more extreme conditions. Moreover, for this long tether architecture, it is possible to study a guidance method for directing the balloon and the whole system using a sail attached at the bottom end of the system. Another important study related to the towing problem is the addition of an autonomous flight object in the system, as representative of an approaching vehicle launched from the surface, necessary for capturing samples of the planet. In the case study presented later, the autonomous flying object is a MAV taken from the literature [22, 23, 24, 25]. The mathematical model used for this study could be either the Lumped-Mass or DeNOC, but for the results shown later the Lumped-Mass is leveraged.

	f_{10} [Hz]	f_{20} [Hz]	f_{50} [Hz]
Lumped-mass	0.133	0.066	0.066
Project Chrono	0.133	0.066	0.066

Table 1: *Analysis of the yaw angle in the frequency domain for the results obtained with the Venus Aerobot Simulator and Project Chrono*

5.1 Validation for long tether analysis

NASA's Jet Propulsion Laboratory has carried out studies using a static model [26] for towing analysis, so comparison with results obtained using the static model are made to validate the developed simulator. In the document taken as a reference [27], many tests with different configurations have been done. However, for this comparison study, only the one chosen in the document as the design configuration is considered. The towed body mass is $m_{body} = 4\ kg$, while the shape considered for the aerodynamic forces is a sphere with the following parameters: $C_d = 0.47$ for the drag coefficient, $d = 0.1m$ for the sphere diameter. For the tether, the following parameters are considered: $l = 9.7\ km$ for the tether length, $m = 2.3\ kg$ for the tether mass, $C_n = 1$ for the normal aerodynamic drag coefficient, $C_t = 0.03$ for the tangential aerodynamic drag coefficient.
For the dynamic simulation using the Lumped-Mass approach, it was necessary to fix the balloon and consider the wind shear acting on the system, not the absolute wind. The comparison is reported in Fig. 15. The differences in the responses are due to the different approaches used. The developed dynamic simulator is more exact, as it includes distributed inertia, elasticity, and aerodynamic loads along the 9.7 km tether. This satisfying result proves that the Venus Aerobot Simulator is capable of simulating configurations with long tethers.

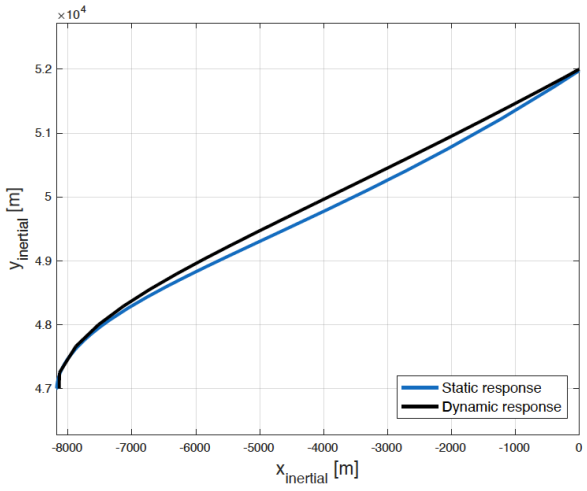

Figure 15: *Static versus Dynamic analysis for towed body*

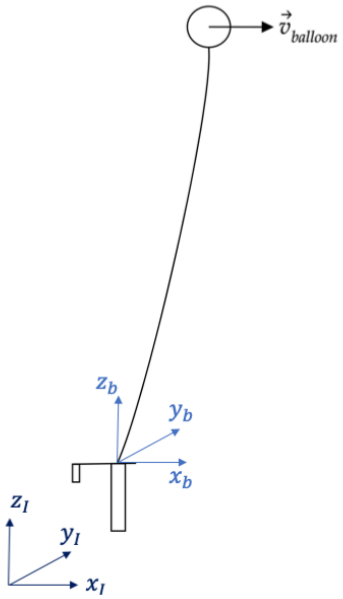

Figure 16: *Scheme of the system used for changing the balloon trajectory*

5.2 Aerobot trajectory control

In past years, studies were done at NASA's Jet Propulsion Laboratory on Earth's applications of a lateral control mechanism for stratospheric platforms [28]. We adopted this concept to exploit the changing wind patterns at different heights to generate passive lateral control forces on a balloon, employing a particular aerodynamic structure attached to the balloon via a tether. The lifting device connected to the end of the tether takes advantage of the variation of the wind velocity with altitude. The winds leveraged for this purpose are the zonal winds, which are more potent than the meridional winds on Venus. This lateral control mechanism leads to interesting applications on Venus, since it has an atmospheric super-rotation, where the atmosphere rotates faster than the planet itself. Since a reasonable requirement for this system would be to have a decent wind shear with altitude, Venus would provide a good environment. The wing immersed in the flux generates a horizontal lift, which will be able to move the balloon as soon as the tether goes in tension, moving the whole system as a consequence. In this way, it would be possible to cover a broader range of atmosphere for a scientific Venus mission, avoid hazards, and reach targets. The magnitude of the trajectory control will depend on the relative sizes of the balloon and the sail design, with the air density and the magnitude of wind velocity between the two altitudes. A simplified representation of the system is shown in Fig. 16.

5.2.1 Mathematical model for the sail

In this section, a more detailed explanation of all the forces involved in the sail system and its dynamics [29] are given. The system that comes into play is shown in Fig. 16. It is clear from Fig. 16 that it is necessary to define a sail reference frame, which will also be called 'body reference frame' in this section. One of the first assumptions is the consideration of symmetric profiles for both the rudder and the main wing, meaning the aerodynamic moment coefficient is equal to zero, $C_m = 0$. The angle of attack of the main wing is calculated using the sail velocities in the body reference frame $\alpha_w = atan\left(\frac{v}{u}\right)$, where u and v are the velocities along the x-axis and y-axis in the body reference frame, as shown in Fig. 17.

The lift coefficient for both the main wing and the rudder is considered linear with the angle of attack, and it could be written in the first approximation as $C_L = 2\pi\alpha$. The drag force is considered only for the main wing and neglected for the rudder. The drag coefficient is non-linear with the lift coefficient C_L, such that $C_D = C_{D_0} + \frac{C_L^2}{\pi\, AR\, e}$.

Lift and drag forces can be seen in Fig. 17. We need to identify the wind reference frame to define aerodynamic forces in the body reference frame.

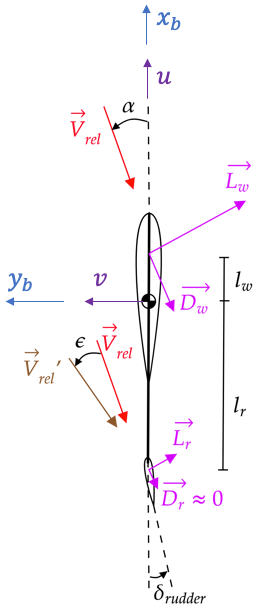

Figure 17: *Flight mechanics sail scheme*

Then, to rotate those forces in the body reference frame, a direction cosine matrix is needed, and this matrix is defined using the angle of attack that occurs both for the main wing and for the rudder. Mathematically, these forces are expressed in the body frame as Eqs. 5.

$$\begin{aligned} \mathbf{L}^{\mathcal{B}} &= \tfrac{1}{2} \cdot \rho_{\text{air}}(z) \cdot ||\mathbf{V}_{\text{rel}}||^2 \cdot C_L \cdot S_{\text{ref}} \cdot \hat{\mathbf{i}}_b \\ \mathbf{D}^{\mathcal{B}} &= -\tfrac{1}{2} \cdot \rho_{\text{air}}(z) \cdot ||\mathbf{V}_{\text{rel}}||^2 \cdot C_D \cdot S_{\text{ref}} \cdot \hat{\mathbf{j}}_b \end{aligned} \tag{5}$$

The force that guides the system through the Venusian atmosphere is best described in the inertial reference frame as the vectorial sum between $\mathbf{L}^{\mathcal{I}}$ and $\mathbf{D}^{\mathcal{I}}$. A rotation using direction cosine matrixes is needed for the definition of lift and drag in the inertial reference frame. Only the projections of the lift and drag force onto the inertial axes are considered since the primary goal is to alter the latitude of the system.
For the rudder angle of attack calculation, the definition of a downwash angle ϵ is necessary. The downwash angle in aerodynamics refers to the downward airflow direction behind a lifting surface, like a wing, caused by the lift generation. It is a critical factor influencing the stability and control of the sail, impacting the effectiveness of control surfaces and overall flight performance. The downwash angle depends on the distance between the main wing trailing edge and the rudder leading edge, but this dependence was neglected for this study. Thus, the rudder angle of attack is computed as $\alpha_{rudder} = \alpha_w - \delta_{rudder} + \epsilon$, where $\epsilon \approx \frac{2C_{L_w}}{\pi AR}$. For this study, the following parameters are used: $AR = 5$, which represents the *aspect ratio* for both the main wing and rudder; $S_{\text{wing}} = 3$ m^2, which represents the *main wing surface area*; $e = 0.7$, which represents the *Oswald efficiency number*, typically between 0.7 and 0.85; $l_w = 0.5$ m, which represents the distance between the sail's center of mass and the main wing's aerodynamic center; $l_r = 4$ m, which represents the distance between the sail's center of mass and the rudder's aerodynamic center.
This is a preliminary study of the feasibility of using a sail to change the trajectory. Another important aspect to discuss is the rotation of the sail about the x_b (x-axis in the body reference frame), also called roll angle, because the lift has a moment arm with respect to the point where the tether is attached. This causes a rotation of the lift direction, modifying the force necessary to guide the entire system. Even though this might be an important aspect to study for the sail efficiency, this rotation was neglected for this study.

5.2.2 *Trajectory control using a proportional controller*

We adopted a simple proportional controller to control the rudder angle δ_e shown in Fig. 17. The rudder lift will be necessary to generate an angle of attack on the main wing that will drive and guide the entire system toward the target latitude. The elementary control law used was the following:

$$\alpha_{rudder} = K_p(y_{commanded} - y) \ , \tag{6}$$

where $y_{commanded}$ and y represent the commanded latitude and the actual latitude, respectively. From a first guess, the proportional gain is $K_p = -\frac{0.1}{180}\frac{\pi}{m}\frac{rad}{m}$. We point out that the latitude in this case is just an example because a North-West-Up reference frame was implemented and not a Venus-Centered Reference frame. The purpose of this study is to demonstrate the feasibility of controlling the balloon's trajectory by utilizing the sail concept on Venus.

5.2.3 Case study

After all the essential considerations done before, a case study on Matlab was made. In this case study, only the zonal wind acting along the x-axis with the intensity varying with the altitude, shown in Fig. 18, is considered. The tether has length $l_t = 2\ km$ with a target latitude of $y_{commanded} = 10\ m$.

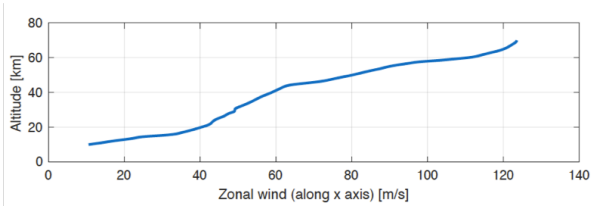

Figure 18: *Venus zonal wind*

The simulation showed that the system tracks the commanded trajectory, albeit with some oscillations due to the used control law, as detailed in Sec. 5.2.2. The system response is shown in Fig. 19.

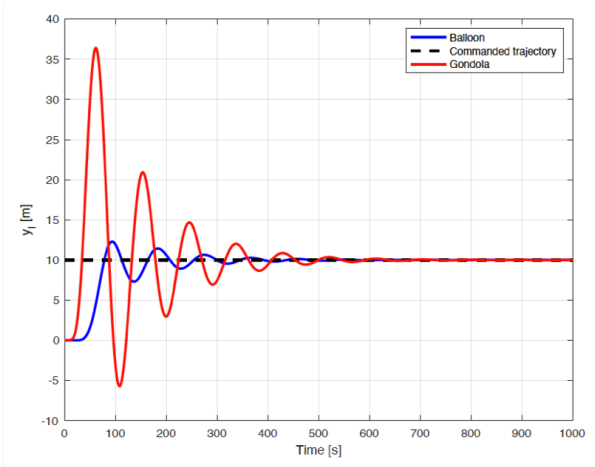

Figure 19: *System response using a proportional controller for the sail rudder*

This study is preliminary, and, if needed, a more detailed analysis using a Venus-Centered Reference Frame can be conducted.

5.3 Tracking and chasing the towed body

Exploring the surface and depths of Venus's atmosphere presents formidable challenges, with its extreme temperatures and pressures shaping a hostile environment unlike any other in our solar system. Drones present an intriguing opportunity for sample collection from the Venusian atmosphere or the high-pressure, high-temperature surface. This feat represents a significant leap forward in our research to understand the mysteries of Venus, offering the possibility of obtaining invaluable data and samples from hardly accessible regions. In this section, the potential of autonomous drone technology to navigate and track the trajectory of towed bodies in the Venusian atmosphere is presented. To simulate the problem, a Simulink model [22, 23, 24, 25] is leveraged. The study is conducted using the system represented in Fig. 16, where a sail is leveraged to alter the trajectory by changing the rudder angle and proving that the drone is able to follow it.

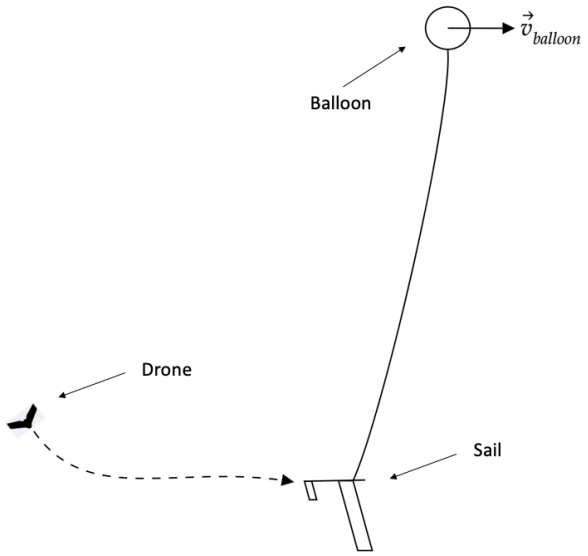

Figure 20: *System conceptual scheme for the simulation that includes the autonomous drone*

The drone interacts with the drogue in the paper taken as a reference [22]. Herein, however, the drone does not interact with the towed body.

5.4 Case study - Drone chasing the gondola

This section presents a case study where a sail is used as a gondola to change the trajectory at a specific time using a constant rudder angle to prove that the drone can chase the gondola trajectory. For this case study, there is one tether with length $2km$, and the rudder angle is described by a step function, which is 0° until $10s$ and 1° between $10s$ and $50s$.
The difference between the position coordinates of the drone and the gondola over time is plotted to

prove that the drone correctly follows the gondola while changing direction. The drone has a starting point not coincident with the gondola starting point at $t = 0\ s$ to ensure a nonzero error at the beginning. The error decreases with time along the inertial y and z coordinates. For the x inertial coordinate, instead, the error tends to a constant value, meaning the drone follows the gondola with a distance offset and is ready to start the docking maneuver, which is not considered in this study. The errors in the coordinates are shown in Fig. 21. Note that a change from the North-West-Up reference frame to the North-East-Down reference frame for the gondola coordinates was needed for leveraging the Simulink model.

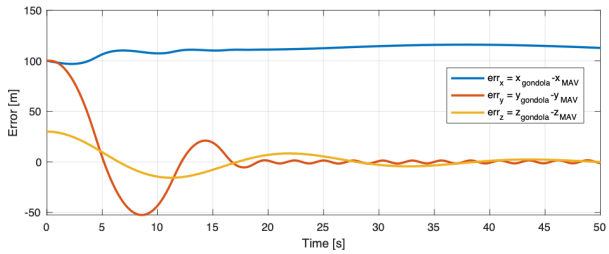

Figure 21: *Error variable over time*

These results confirm the feasibility of adding an autonomous drone in the system, which could also be representative of a surface-launched drone or used to take samples from a broader atmosphere range using faster dynamics. More detailed studies of the docking phase will be made in the future.

6. Conclusions

The development of the Venus Aerobot flight simulator described in this paper has been instrumental in enabling preliminary system-level analysis and enhancing our understanding of the aerobot's flight dynamics. This simulation tool has proven essential for analyzing multiple mission architectures and efficiently optimizing system parameters.

The simulator's **versatility** and **adaptability** have enabled the exploration of a wide range of test cases, providing a robust foundation for subsequent system design studies. The **modularity** of the code has facilitated the seamless integration of additional features throughout the development process, highlighting the potential for further enhancements in future iterations.

The comparative analysis of the DeNOC and Lumped-Mass modeling approaches yielded highly favorable results, suggesting promising avenues for employing the DeNOC robotic-based approach in the modeling of tethered systems, considered as examples of continuum manipulation systems. This finding has significant implications for advancing the field of tethered system dynamics.

Validation efforts, supported by studies and reference materials, have reinforced the reliability of the Venus Aerobot Simulator's outcomes. Initial validation studies using the open-source multi-physics simulation engine *Project Chrono* have produced promising results, which are detailed in this research.

Extensive sensitivity analyses were conducted to delineate the simulator's limitations and ensure the accuracy of the results through comparison with simple models and physical principles.

Finally, the demonstrated feasibility of altering the balloon's trajectory through the use of a sail as an control actuation mechanism for the aerobot opens new avenues for lateral control of the system, offering exciting prospects for future research and development.

Acknowledgements

This research was carried out at Jet Propulsion Laboratory, California Institute of Technology under a contract with the National Aeronautics and Space Administration (80NM0018D0004), as part of the JPL Visiting Student Research Program that hosted Mr. Vergari and Mr. De Matteis under the mentorship and supervision of Dr. Quadrelli, Dr. Rossi, and Dr. Blomquist at JPL, and of Prof. Romano, Mr. Apa, and Mr. Aliberti at Politecnico di Torino. The authors are grateful to the other JPL members of the Venus Aerobot Team (Dr. James Cutts, Dr. Jacob Izraelevitz, Dr. Ashish Goel, Mr. Len Dorsky, and Dr. Kim Aaron) for very useful discussions.

The participation of Riccardo Apa was supported by the project NODES which has received funding from the MUR – M4C2 1.5 of PNRR funded by the European Union - NextGenerationEU (Grant agreement no. ECS00000036), and the participation of Dr. Marcello Romano was partially supported by a grant of Compagnia di San Paolo.

References

[1] European Space Agency. How venus and mars can teach us about earth, 2024. URL `https://www.esa.int/Science_Exploration/Space_Science/How_Venus_and_Mars_can_teach_us_about_Earth`. Accessed: 2024-08-30.

[2] NASA Jet Propulsion Laboratory. Venus variable altitude aerobots, 2023. URL `https://www-robotics.jpl.nasa.gov/what-we-do/research-tasks/venus-variable-altitude-aerobots/`. Accessed: 2024-08-30.

[3] Linskens H. T. K. and Mooij E. Tether dynamics analysis and guidance and control design for active space-debris removal. *Journal of Guidance, Control, and Dynamics*, 39(6), 2016.

[4] S. Saha. Dynamics of serial multibody systems using the decoupled natural orthogonal complement matrices. *Journal of Applied Mechanics*, 66:986–996, December 1999.

[5] Jeffery L. Hall, Michael T. Pauken, Aaron Schutte, Siddharth Krishnamoorthy, Carolina Aiazzi, and Jacob S. Izraelevitz. Prototype development of a variable altitude venus aerobot. In *AIAA AVIATION Forum*, Virtual Event, August 2021.

[6] Jeffery L Hall, Jonathan Cameron, Michael Pauken, Jacob Izraelevitz, Mitchell W Dominguez, and Kristopher T Wehage. Altitude-controlled light gas balloons for venus and titan exploration. In *AIAA Aviation 2019 Forum*, page 3194, 2019.

[7] Martha S. Gilmore, Patricia M. Beauchamp, Richard Lynch, and Michael J. Amato. 2020 venus flagship mission study. Technical report, Planetary and Astrobiology Decadal Survey, August 2020.

[8] Valentina Lo Gatto, Jacob S. Izraelevitz, Michael T. Pauken, Ashish Goel, Rebekah Lam, and Jeffery L. Hall. Inflation sequence tradeoffs and laboratory demonstration of a prototype variable-altitude venus aerobot. *Acta Astronautica*, January 2024.

[9] P. Williams. Cable modeling approximations for rapid simulation. *Journal of Guidance, Control, and Dynamics*, 40(7), July 2017.

[10] Bong W. *Space Vehicle Guidance Control and Astrodynamics*. AIAA Education Series, 3rd ed. edition.

[11] J. Virgili, J. V. Drew II, and M. Romano. Spacecraft robotics toolkit: an open-source simulator for spacecraft robotic arm dynamic modeling and control. In *6th International Conference on Astrodynamics Tools and Techniques (ICATT)*, Darmstadt, 2021. GitHub source: `https://github.com/NPS-SRL/SPART`.

[12] S. Saha. A decomposition of the manipulator inertia matrix. *Robotics and Automation, IEEE Transactions on*, 13:301–304, April 1997.

[13] A.H. Techet. Hydrodynamics. TA B. P. Epps.

[14] Williams P., Sgarioto D., and Trivailo P. Motion planning for an aerial-towed cable system. In *AIAA Guidance, Navigation, and Control Conference and Exhibit*, San Francisco, California, 2005.

[15] Faith A. Morrison. Data correlation for drag coefficient for sphere. Technical report, Department of Chemical Engineering, Michigan Technological University, Houghton, MI, November 2016.

[16] A. Martinez, S. Lebonnois, E. Millour, T. Pierron, E. Moisan, G. Gilli, and F. Lefèvre. Exploring the variability of the venusian thermosphere with the ipsl venus gcm. *Icarus*, 389: 115272, January 2023.

[17] S. Lebonnois, N. Sugimoto, and G. Gilli. Wave analysis in the atmosphere of venus below 100-km altitude, simulated by the lmd venus gcm. *Icarus*, 2016.

[18] S. Lebonnois, F. Hourdin, V. Eymet, A. Crespin, R. Fournier, and F. Forget. Superrotation of venus' atmosphere analyzed with a full general circulation model. *Journal of Geophysical Research*, 115(E6):E06006, 2010.

[19] B. Camilla. Stochastic wind gust model for

aerobot in venus atmosphere. Master's thesis, Polytechnic University of Turin, 2024.

[20] M. Quadrelli, L. Dorsky, J. Izraelevitz, A. Goel, R. Blomquist, E. Marteau, and J. Cutts. Modeling, analysis, and design of dynamic couplings in planetary tethered aerobot systems. In *Interplanetary Probe Workshop*, Williamsburg, VA, June 8–14 2024.

[21] A. Tasora, R. Serban, H. Mazhar, A. Pazouki, D. Melanz, J. Fleischmann, M. Taylor, H. Sugiyama, and D. Negrut. Chrono: An open-source multi-physics dynamics engine. *High-Performance Computing in Science and Engineering-Lecture Notes in Computer Science*, pages 19–49, 2016.

[22] Mark B. Colton, Liang Sun, Daniel C. Carlson, and Randal W. Beard. Multi-vehicle dynamics and control for aerial recovery of micro air vehicles. *International Journal of Vehicle Autonomous Systems*, 9(1/2), 2011.

[23] J. W. Nichols and L. Sun. Autonomous aerial rendezvous of small unmanned aircraft systems using a towed cable system. In *43rd Annual Society of Flight Test Engineers Symposium*, October 2012.

[24] Randal W. Beard and Timothy W. McLain. *Small Unmanned Aircraft: Theory and Practice*. Princeton University Press, 2012.

[25] Hassan K. Khalil. *Nonlinear Systems*. Prentice Hall, 2002.

[26] M. S. Triantafyllou and F. S. Hover. *Maneuvering And Control Of Marine Vehicles*. Department of Ocean Engineering, Massachusetts Institute of Technology, Cambridge, Massachusetts, USA.

[27] P. McGarey, B. Hockman, B. Sutin, J. Izraelevitz, Anthony Davis, J. Cutts, L. Dorsky, and K. Baines. A tethered towbody payload for inand sub-cloud sensing on venus. In *IPPW 2021*, 2021.

[28] K. M. Aaron, M. K. Heun, and K. T. Nock. A method for balloon trajectory control. Technical report, Global Aerospace Corporation, 711 West Woodbury Road, Suite H, Altadena, CA 91001-5327, USA.

[29] Christopher D. Yoder, Thomas R. Gemmer, and Andre P. Mazzoleni. Modelling and performance analysis of a tether and sail-based trajectory control system for extra-terrestrial scientific balloon missions. *Acta Astronautica*.